3D-Printed Guides in Bone Tumor Resection: Studying Their Error and Determining a Safety Margin for Surgery

VAMIQ M. MUSTAHSAN, MS; CARLOS G. HELGUERO, PHD; GUANGYU HE, MS; DAVID E. KOMATSU, PHD; DEREK HANSEN, MD; SRINIVAS PENTYALA, PHD; IMIN KAO, PHD; FAZEL KHAN, MD

abstract

3D-printed guides, which have recently been introduced in orthopedic oncology, improve resection accuracy compared with traditional bone resection methods, but there are inaccuracies associated with them. These inaccuracies could lead to disastrous outcomes such as positive tumor resection margins. In this Sawbone study, we sought to quantitatively investigate the margin of error for various jig types and to determine a "safety margin" that could serve as a guide for surgeons and jig engineers in creating 3D-printed jigs that would reduce the risk of potential disastrous results such as positive margins. Various 3D-printed jigs were used to simulate wide resection of a distal femoral bone sarcoma on Sawbone specimens by 10 individuals with no specific prior expertise in cutting guides. We developed a mathematical model using kinematic theory. We defined a safety margin as the amount of change in the osteotomy lines that must be incorporated into the jig design to ensure that the surgeon is at least 98% likely not to have a positive tumor margin. Experiments were conducted to determine the mean deviation experienced in placing cutting guides on the bones. The mean deviation for the four types of cutting guides ranged from 2.86 mm to 6.54 mm. We determined that a jig design should have a safety margin of 4.8 mm for standard guides and 8.65 mm for gusset guides to minimize the possibility of cutting into the tumor as a result of human error in guide placement. Further studies involving cadavers and patients are warranted. [*Orthopedics*. 2022;45(3):169-173.]

The surgical treatment of bone tumors using computer-generated cutting guides has been shown to be more accurate than traditional freehand resections.[1,2] However, previous studies by our group have shown that there are certain finite errors in resection accuracy associated with this technique.[3] Our previous data suggest that the majority of the cutting errors that are present with 3D-printed jigs are related to human error when the surgeon positions the jig on the bone.[4] Although the jigs are designed to fit in only one configuration on the bone, there is always some practical ambiguity on the part of the surgeon regarding where exactly to place the jig.[5,6] As a result, the preoperative resection plan is not reproduced exactly as desired at the time of the procedure.[7,8] This could potentially lead to positive margins during surgery for cancer, which can have devastating local and systemic oncologic consequences. Additionally, if a custom implant is designed preoperatively to fit into the expected skeletal defect left after a bone tumor resection, such errors could lead

The authors are from the Department of Mechanical Engineering (VMM, GH, IK), Stony Brook University, and the Department of Orthopedics (DEK, DH, FK) and the Department of Anesthesiology (SP), Stony Brook Medical Center, Stony Brook, New York; and the Department of Mechanical Engineering and Production Sciences (CGH), ESPOL Polytechnic University, Guayaquil, Ecuador.

The authors have no relevant financial relationships to disclose.

The authors thank Stony Brook Cancer Center and Mr Charles Mazzarese for supporting them in procuring computed tomography scans for this study.

Correspondence should be addressed to: Vamiq M. Mustahsan, MS, Department of Mechanical Engineering, Stony Brook University, 113 Light Engineering Bldg, Stony Brook, NY 11794 (vamiq.6@gmail.com).

Received: October 27, 2020; Accepted: May 9, 2021; Posted online: February 22, 2022.

doi: 10.3928/01477447-20220217-05

Table 1
Terminology Used in Modeling

Kinematic terminology	Anatomical terminology
XY plane	Coronal plane
YZ plane	Transverse plane
ZX plane	Sagittal plane
X axis (X_o)	Longitudinal axis
Y axis (Y_o)	Frontal axis
Z axis (Z_o)	Sagittal axis

to improper fit of the implant, potentially rendering it useless.

Accuracy when performing a guided resection has been found to depend on preoperative and in vivo factors. The preoperative factors include the error accumulated in conversion from DICOM images of a computed tomography (CT) scan to a NURBS-based 3D CAD model; and the resolution of the 3D printer, which affects the fabrication of the cutting guide that is required to perfectly match the surface topology of the bone. The in vivo factors include the soft tissue on the bone during surgery, which affects guide placement; and the surgeon's guide placement and saw orientation while performing the resection.

It is essential that we study the extent of the cumulative effects of these factors on guided resection and improve overall accuracy. In this article, we describe development of a kinematic model of the resection procedure that enables us to mathematically quantify the error in jig placement by calculating the deviation from the preoperative path in surgery. This allows empirical determination of the maximum error that should be incorporated as a margin of safety in the design of the cutting guide.

Materials and Methods

Kinematic Modeling

We developed a mathematical model that will be used to determine the deviation of path based on the relative positioning of the bone and the cutting guide. We defined two coordinate frames, frame {B} and frame {J}, which are fixed to the bone and cutting guide, respectively [**Figure A(a)**, available in the online version of the article]. Both frames are defined with respect to a global inertial reference frame {O}, with the origins defined as displacement vectors $\vec{\mathbf{p}}_b$ and $\vec{\mathbf{p}}_j$, respectively, in frame {O}, for the bone and guide. **Table 1** describes the global coordinate frame {O} in anatomical terms.

Any point in this model can be represented as a position vector $\vec{\mathbf{r}}_j$ and $\vec{\mathbf{r}}_b$ with respect to frame {J} and {B}, respectively [**Figure A(b)**]. The relationship between these two vectors is expressed as,[9,10]

$$\vec{\mathbf{r}}_j = {}^{J}_{B}\mathbf{H}\,\vec{\mathbf{r}}_b \qquad (1)$$

where ${}^{J}_{B}\mathbf{H}$ is a 4x4 transformation matrix expressed as,

$${}^{J}_{B}\mathbf{H} = \begin{bmatrix} {}^{J}_{B}\mathbf{R} & \vec{\mathbf{p}}_{bj} \\ 0\ \ 0\ \ 0 & 1 \end{bmatrix} \qquad (2)$$

where the vector $\vec{\mathbf{p}}_{bj}$ is the displacement of origin of frame {J} with respect to frame {B} representing translations (Δx, Δy, Δz) of the guide and the rotation matrix, ${}^{J}_{B}\mathbf{R}$, represents the rotations of frame {J} with respect to frame {B} representing roll (α), pitch (β), and yaw (γ) (**Figure B**, available in the online version of the article).

Using ${}^{J}_{B}\mathbf{H}$, we can mathematically track the deviation of every point on the cutting path from its ideal position on the bone based on the change in guide placement.[9]

Design and Positioning of the Cutting Guide

The cutting guide was designed using major anatomical landmarks on the bone. One such feature is the curve formed by the superior ridge of the medial femoral articular surface, $\mathbf{C}_B$. The projection of $\mathbf{C}_B$ on the cutting guide is $\mathbf{C}_G$ [**Figure C(a)** and **Figure C(c)**, available in the online version of the article]. Another feature is the surface topology of the bone itself, which was copied on the underside of the guide to provide more stability in the placement process. During surgery, the superior ridge was exposed and bone landmarks were aligned with ones found on the guide (**Figure C**).[4] When the surgeon was confident in the placement, the guide was fixed into position using three Steinmann pins.

Determination of Safety Margin for Preoperative Path

Considering the tumor to be an ellipsoid volume [**Figure D(a)**, available in the online version of the article], we outline a cutting path $\overline{ABCD}$ on the outer boundary of the ellipsoid tumor as the ideal path on the bone. Based on $\overline{ABCD}$, we designed the cutting path $\overline{A'B'C'D'}$ on the jig [**Figure C(a)** and **Figure C(b)**]. However, in the operating room, when positioning of the cutting guide is not perfect because of factors described earlier, the path $\overline{A'B'C'D'}$ deviates from $\overline{ABCD}$. Even a small deviation from the ideal resection path may cause the surgeon to cut through the tumor margin, which can be catastrophic. To prevent this, we define a margin of safety that will be used in preoperative planning so that small deviations do not lead to medical complications.

To determine the safety margin, we find the maximum rotational error along all three axes (ie, roll, pitch, and yaw) and also the maximum translational error when positioning the jig. Using this relationship, ${}^{J}_{B}\mathbf{H}$ from equation 1, we track the position of every point in the cutting path designed on the guide with respect to the ideal path traced on the bone. We express this deviation in the cutting path resulting from incorrect positioning of the guide as positioning error of the guide (e). The derivation and calculation of the positioning error is explained in detail in **Table A** (available in the online version of the article).

Because the surgeon performs resection by moving the saw along the sagittal (Z) axis (because $\overline{A'B'C'D'}$ is on the coronal [XY] plane), we calculate the magnitude of largest error vector projection of $\vec{\mathbf{e}}$ on the coronal plane empirically. A new cutting path $\overline{FGHI}$ extended by a safety margin of

(e) from $\overline{A'B'C'D'}$ is constructed as the desired cutting path [**Figure D(b)**]. This new preoperative path will significantly reduce the possibility of positive margins.

Empirically Determining the Safety Margin

Based on the kinematic model of the jig placement, we empirically determined the mean deviation in all 6 degrees of freedom ($\alpha, \beta, \gamma, \Delta x, \Delta y$, and Δz) of the cutting guide. Because we are dealing with high-risk surgeries that may lead to metastasis or death, we define the margin to be the mean value of deviation and two standard deviations of the empirical values obtained so that the surgeon is 98% likely not to cut into the tumor.

Fabrication of Cutting Guides

We converted the CT scan DICOM images of femur bones (Sawbones) into a 3D CAD model of the bone using the 3D conversion process described by Helguero et al.[4] Extracting the surface of the bone and assuming a 10x10x25-mm ellipsoid to be the tumor, we designed the cutting path [**Figure D(a)**]. Four types of cutting guides were designed and fabricated using a Cubify 2nd Generation Cube 3D (3D Systems) printer (**Figure E**, available in the online version of the article), with each one having unique features enabling it to be better suited for different cases of resection. The four types of cutting guides were as follows: (1) standard—a guide with no extra features, similar to the guides used in our earlier experiments[4]; (2) standard with gusset—the standard guide with a gusset feature at the top as an added constraint; (3) surface with distributed spikes—the guide with multiple miniature spikes randomly distributed throughout its surface that penetrate the soft tissue and touch the bone surface (the concatenation of all of the tips forms the bone surface); and (4) surface with distributed spikes and gusset—the standard guide including spikes on the surface and a gusset.

Positioning Study

Ten different surgeons or trainees with no previous training on guide positioning were asked to place the four types of guides over the femur bone surface under the following two conditions: (1) a clean and smooth surface and (2) a simulated tissue-covered surface.

These two conditions help us in determining the effect of soft tissue in guide placement. Soft tissue is simulated by randomly covering the surface of Sawbones with modeling clay. After positioning, the setup was CT scanned to quantify the relative position of the guide with respect to the Sawbone femur.

Quantifying Degrees of Freedom

Quantify rotations (α, β, γ)

Each experiment was analyzed using CT scans to accurately calculate the relative rotation of the cutting guide with respect to the surface of the bone. The coordinate axis for the bone, frame {B}, was defined with the help of anatomical landmarks on the Sawbone; these landmarks also act as a fixed reference while calculating the orientation of the cutting guide. The plane formed by the three points P1, P2, and P3, which are centers of fiducial pins in the CAD solid model on the cutting guide, and the direction of normal to this plane at the centroid of the triangle formed by P1, P2, and P3 ($\vec{m}$) were used to define frame {J} (**Figure F**, available in the online version of the article). Angles α and β were obtained by projecting the vector $\vec{\mathbf{m}}$, normal to the defined plane, onto the transverse (YZ) and sagittal (ZX) planes of frame {B}, respectively. The angle between the axial cutting slot in the coronal (XY) plane of frame {B} was used to calculate γ [**Figure F(a-d)**].

Quantify translation errors about the X, Y, and Z axes (Δx, Δy, and Δz)

Coordinates of the centroid of this triangle formed by the centers of fiducial holes (P1, P2, and P3) were considered as the origin of frame {J} [**Figure F(e)**]. The change in position of the centroid from the ideal location was considered as the translation error in the coronal (XY) plane. During positioning, the surgeon presses the cutting guide against the bone surface along the negative Z direction (sagittal axis) [**Figure F(f)**]. Therefore, part of the cutting guide is in contact with the bone surface and the rest is displaced due to randomly distributed soft tissue, resulting mainly in pitch displacement. In addition, because the saw movement is in the negative Z direction, the Z translation of the guide does not play a significant role in the deviation of resection path.

RESULTS

The means and standard deviations of roll (α), pitch (β), and yaw (γ) in each experiment were obtained. **Table 2** lists the rotation errors of the cutting guide for smooth bone and tissue-covered bone. These results indicate that the magnitude of rotation error does not exceed a mean of 5° in all cases.

Table 3 lists the translation errors along the longitudinal (X) axis and the frontal (Y) axis on smooth bone and tissue-covered bone, respectively. We consider the Z translation error to be 0 mm in the case of smooth bone and 1 mm in the case of tissue-covered bone.

Applying the Kinematic Model to Calculate Errors for a Wide Resection of Osteosarcoma

As explained earlier, we designed a cutting path as shown in **Figure D**. We selected 8 corner points on the preoperative resection path on the upper side and the lower side of the bone. With the measured values of α, β, γ, Δx, Δy, and Δz from the experiments, we calculated the errors of deviation of cutting path ($\vec{\mathbf{e}}$) for each type of guide (**Table 4**). We finally can determine the safety margin for every type of guide by calculating the maximum error ($\vec{\mathbf{e}}$), defined earlier.

DISCUSSION

Based on the kinematic model, we have performed experiments to quantify the translation and rotation errors of various types of guides. Our results indicate

Table 2

Errors in Rotation After Positioning the Cutting Guides on the Smooth Surface and Tissue-Covered Surface of Bone

	Smooth surface of bone, mean±SD			Tissue-covered surface of bone, mean±SD		
Cutting guide	Roll	Pitch	Yaw	Roll	Pitch	Yaw
Standard	-2.78°±1.35°	-1.39°±1.92°	-3.45°±2.26°	-1.31°±3.20°	-1.60°±1.57°	-4.12°±2.34°
Gusset	-4.45°±1.85°	1.26°±2.16°	-4.26°±0.63°	-3.06°±1.47°	1.67°±1.26°	-4.55°±0.62°
Spike	-2.45°±1.49°	3.27°±1.81°	-3.34°±1.5°	-1.90°±2.06°	3.42°±1.76°	-2.21°±1.84°
Spike and gusset	-2.30°±1.75°	2.09°±1.24°	-1.89°±1.05°	-2.32°±1.83°	1.38°±1.67°	-1.69°±1.37°

Table 3

Errors in Translation After Positioning the Cutting Guides on the Smooth Surface and Tissue-Covered Surface of Bone

	Smooth surface of bone, mean±SD, mm		Tissue-covered surface of bone, mean±SD, mm	
Cutting guide	Longitudinal axis	Frontal axis	Longitudinal axis	Frontal axis
Standard	-1.55±0.96	-1.41±1.54	-1.62±0.96	-2.78±2.45
Gusset	-0.45±1.78	0.76±1.16	-0.56±2.78	0.89±1.89
Spike	-1.15±1.77	1.34±1.25	-1.18±1.77	1.04±0.87
Spike and gusset	-0.73±2.62	2.36±2.97	-0.75±2.62	2.06±0.99

Table 4

Displacement of the Extreme Points on the Preoperative Path and Corresponding Safety Margin

	Smooth surface of bone		Tissue-covered surface of bone		
Cutting guide	Mean±SD, mm	Safety margin, mm	Mean±SD, mm	Safety margin, mm	Pearson correlation
Standard	2.75±1.40	5.55	2.86±1.87	6.60	0.984
Gusset	5.02±2.07	9.16	6.54±2.11	10.76	0.972
Spike	5.36±2.01	9.38	4.34±1.71	7.76	0.999
Spike and gusset	7.10±1.26	9.62	4.85±1.08	7.01	0.981

that the maximum angle of deviation was less than 5° in all cases and translation error was less than 3 mm (**Table 3**).

The mean deviations in the cutting path obtained for each of these guides and their corresponding safety margin (*e*) for customized wide resection are presented in **Table 4**. The safety margin depends on the tissue on the bone surface and the type of jig and ranges from 5.55 mm to 10.76 mm.

Comparing the errors on a smooth surface with those on a tissue-covered surface, we found a consistent increase in mean errors for the guides with no spikes (2.75 mm to 2.86 mm without gusset and 5.02 mm to 6.45 mm with gusset) and a consistent decrease in mean errors for the guides with spikes (5.36 mm to 4.34 mm without gusset and 7.10 mm to 4.85 mm with gusset) (**Table 4**). For the two guides without spikes, we observed reduced contact with the bone when there was randomly distributed tissue compared with guides with spikes, because the spikes pierce through the tissue and conform better to the surface of the bone. This indicates that the randomly distributed soft tissue is a key factor in human error in guide placement. Therefore, in cases with more soft tissue, the guide with spikes may be more desirable.

Although gussets have shown higher mean positioning error (6.54 mm) compared with standard guides (2.86 mm), there are some cases in which adding a gusset may be desirable. For example, if some part of the soft tissue is compromised because of the tumor, a guide with a gusset could be used without touching the soft tissue.

There were several limitations to this study. The use of Sawbones and modeling clay to simulate bone and soft tissue cannot completely reproduce the exact environment of surgery, where skin, muscles, blood, and other factors influence exposure and visibility. Another limitation was that we only considered one type of bone region with a similar type of cut. In light of this, we developed four guides of vary-

ing design to test the positioning. Other designs of cutting guides may be used for different cuts at different locations. Another limitation of this study was that the surgeons had varying levels of training to place the guides. Surgeons with prior experience placing guides, as well as strictly attending-level surgeons, may have demonstrated improved accuracy and precision. Furthermore, when customized jigs are currently used in orthopedic oncology procedures, surgeons are sometimes given a see-through acrylic model with etched laser lines that allows them to "practice" placing the jig in the correct position prior to surgery.[11] This did not happen in this study, potentially influencing the results. The results of this study may reflect more of a worst-case scenario than true means of cutting jig errors in orthopedic oncology surgeries.

Conclusion

The safety margin that we obtained was calculated such that a surgeon is 98% likely not to have positive margins in resection. The incorporation of safety margin in jig design can help the surgeon maintain higher confidence in jig placement during surgery.

References

1. Khan FA, Lipman JD, Pearle AD, Boland PJ, Healey JH. Surgical technique: computer-generated custom jigs improve accuracy of wide resection of bone tumors. *Clin Orthop Relat Res*. 2013;471(6):2007-2016. https://doi.org/10.1007/s11999-012-2769-6 PMID:23292886
2. Fitz W. Unicompartmental knee arthroplasty with use of novel patient-specific resurfacing implants and personalized jigs. *J Bone Joint Surg*. 2009;91(suppl 1):69-76. https://doi.org/10.2106/JBJS.H.01448
3. Cho HS, Oh JH, Han I, Kim H-S. Joint-preserving limb salvage surgery under navigation guidance. *J Surg Oncol*. 2009;100(3):227-232. https://doi.org/10.1002/jso.21267 PMID:19330812
4. Helguero CG, Kao I, Komatsu DE, et al. Improving the accuracy of wide resection of bone tumors and enhancing implant fit: a cadaveric study. *J Orthop*. 2015;12(suppl 2):S188-S194. https://doi.org/10.1016/j.jor.2015.10.010 PMID:27047222
5. Stronach BM, Pelt CE, Erickson J, Peters CL. Patient-specific total knee arthroplasty required frequent surgeon-directed changes. *Clin Orthop Relat Res*. 2013;471(1):169-174. https://doi.org/10.1007/s11999-012-2573-3 PMID:22956239
6. Ramirez MA, Means KR Jr. Digital soft tissue trauma: a concise primer of soft tissue reconstruction of traumatic hand injuries. *Iowa Orthop J*. 2011;31:110-120. PMID:22096429
7. Cartiaux O, Paul L, Docquier P-L, et al. Accuracy in planar cutting of bones: an ISO-based evaluation. *Int J Med Robot*. 2009;5(1):77-84. https://doi.org/10.1002/rcs.237 PMID:19172588
8. Cartiaux O, Docquier P-L, Paul L, et al. Surgical inaccuracy of tumor resection and reconstruction within the pelvis: an experimental study. *Acta Orthop*. 2008;79(5):695-702. https://doi.org/10.1080/17453670810016731 PMID:18839378
9. Siciliano B, Khatib O. *Springer Handbook of Robotics,* 2nd ed. Springer International Publishing; 2016. https://doi.org/10.1007/978-3-319-32552-1
10. Arauz P, Sisto SA, Kao I. Experimental study of the optimal angle for arthrodesis of fingers based on kinematic analysis with tip-pinch manipulation. *J Biomech*. 2016;49(16):4009-4015. https://doi.org/10.1016/j.jbiomech.2016.10.047 PMID:27825603
11. Onkos Surgical. My3D. Accessed February 15, 2021. https://onkossurgical.com/my3d-technologies.

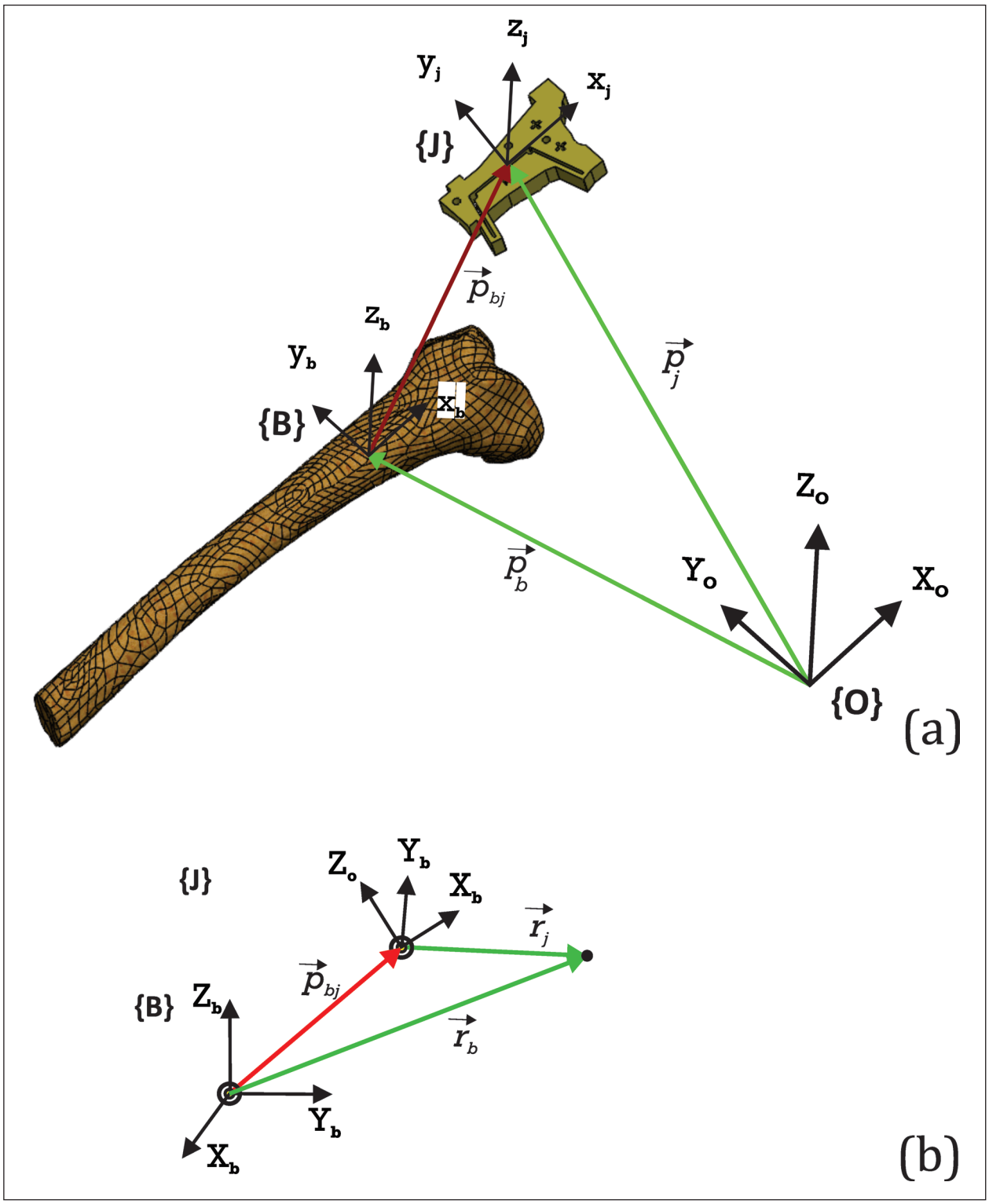

Figure A: (a) Kinematic representation of the setup. The bone and cutting guide (jig) being represented as local coordinate frames ({B} & {J}) defined in relationship with a global coordinate frame {O}; (b) The bone reference frame {B} and guide reference frame {J} are representing the same point by their respective position vectors $\vec{\mathbf{r}}_j$ and $\vec{\mathbf{r}}_b$.

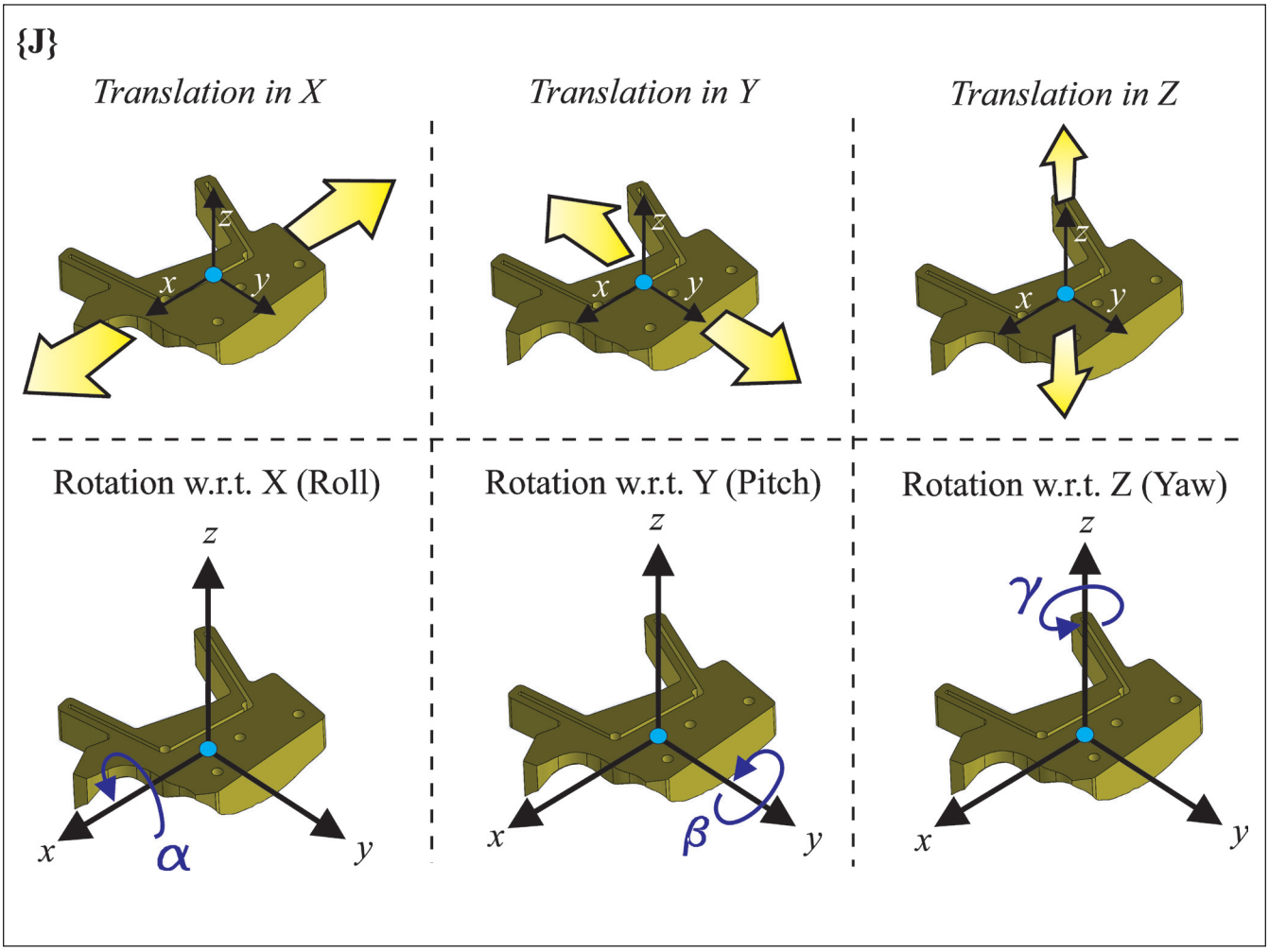

Figure B: Cutting guide as a rigid body, having 6 degrees of freedom in the space; including three translations in the X, Y, and Z directions and three rotations of roll, yaw, and pitch.

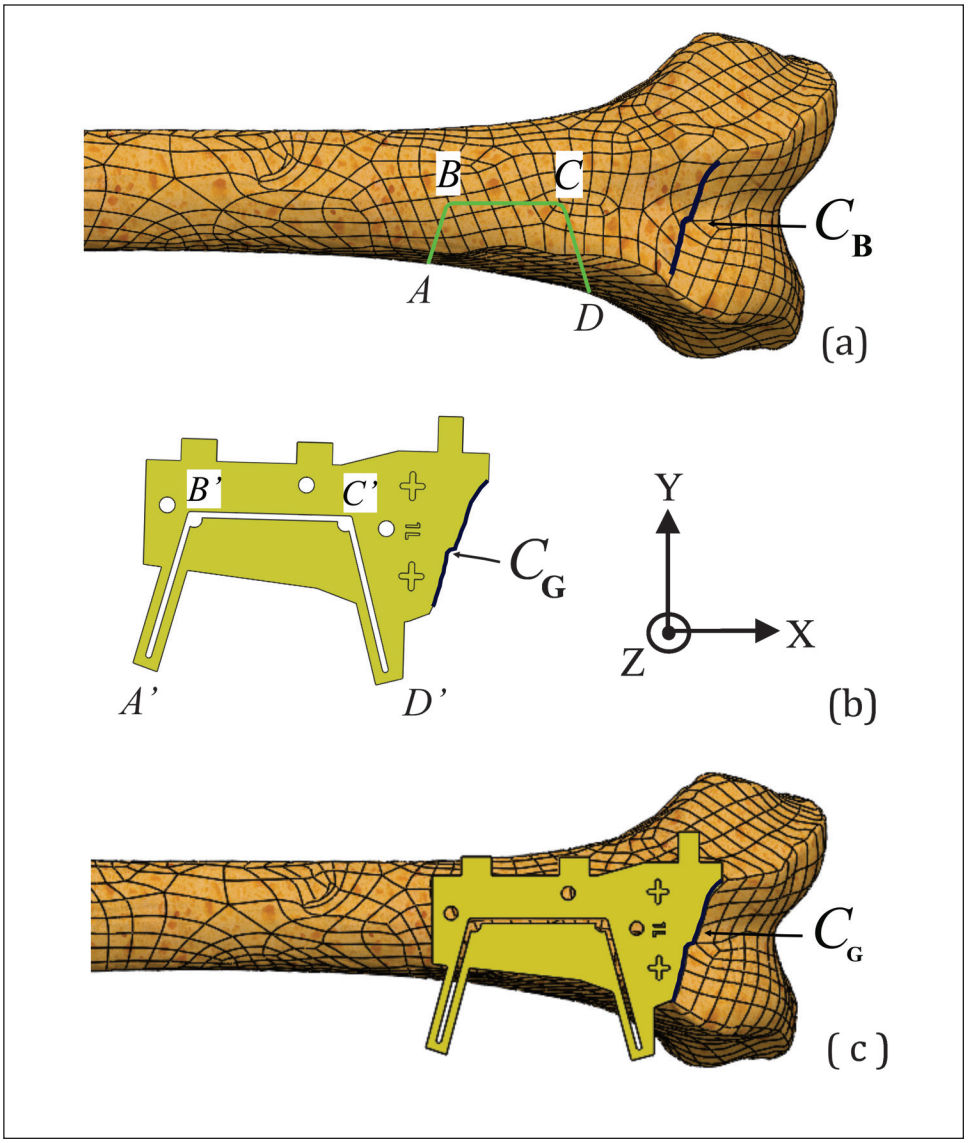

Figure C: (a) Determination of initial cutting path $\overline{ABCD}$ for wide resection based on the outer boundary of the tumor and tracing the curve $\mathbf{C}_B$ on the superior ridge. (b) Design of the cutting guide by copying the curve $\mathbf{C}_B$ onto the guide as $\mathbf{C}_G$along with the cutting path $\overline{A'B'C'D'}$. (c) Ideal placement of the cutting path such that $\mathbf{C}_B$ and $\mathbf{C}_G$ align perfectly.

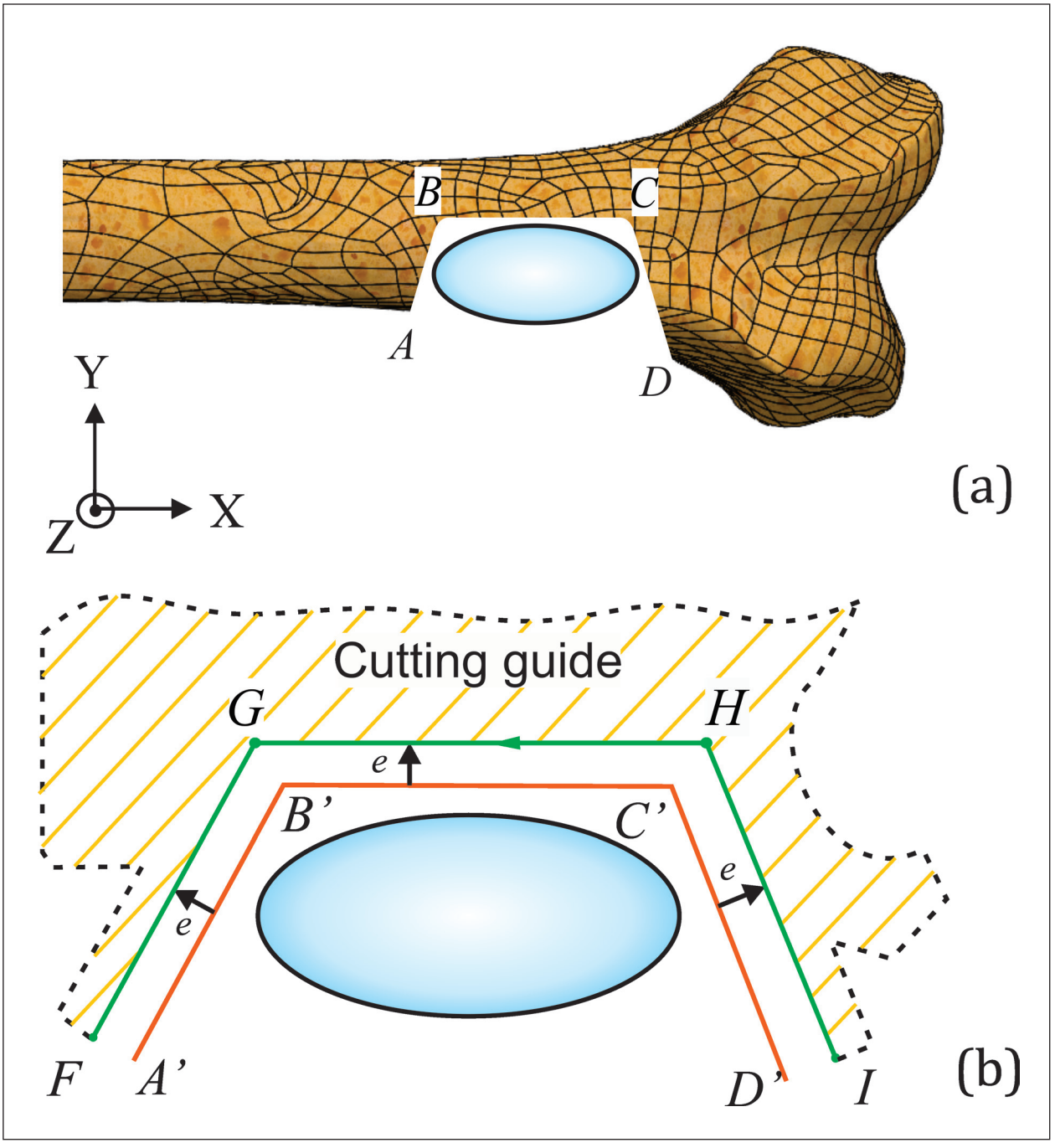

Figure D: (a) Tumor simulated as an ellipsoid and the cutting path $\overline{ABCD}$ designed based on the tumor boundary. (b) New cutting path $\overline{FGHI}$ designed considering the safety margin (e) possible due to improper positioning.

Table A. Positioning error

If $\vec{\mathbf{r}}_j$ is the vector that defines the position of a point on the resection path with respect to frame {J}, and $\vec{\mathbf{r}}_b$ is the same point expressed with respect to frame {B}, we can write

$$\vec{\mathbf{r}}_j = \begin{bmatrix} x_j \\ y_j \\ z_j \\ 1 \end{bmatrix} \qquad \vec{\mathbf{r}}_b = \begin{bmatrix} x_b \\ y_b \\ z_b \\ 1 \end{bmatrix} \tag{3}$$

Any point on the rigid body can be represented as a position vector $\vec{\mathbf{r}}_j$ and $\vec{\mathbf{r}}_b$, with respect to frame {J} and {B}, respectively. From equation 1 and 2, these two vectors are related by a 4 x 4 transformation matrix ${}^{J}_{B}\mathbf{H}$.

$$\vec{\mathbf{r}}_j = {}^{J}_{B}\mathbf{H}\, \vec{\mathbf{r}}_b \tag{4}$$

or

$$\begin{bmatrix} x_j \\ y_j \\ z_j \\ \mathbf{1} \end{bmatrix} = \begin{bmatrix} c\alpha\, c\beta & c\alpha\, s\beta\, s\gamma - s\alpha\, c\gamma & c\alpha\, s\beta\, c\gamma + s\alpha\, s\gamma & \Delta x \\ s\alpha\, c\beta & s\alpha\, s\beta\, s\gamma + c\alpha\, c\gamma & s\alpha\, s\beta\, c\gamma - c\alpha\, s\gamma & \Delta y \\ -s\beta & c\beta\, s\gamma & c\beta\, c\gamma & \Delta z \\ 0 & 0 & 0 & 1 \end{bmatrix} \begin{bmatrix} x_b \\ y_b \\ z_b \\ 1 \end{bmatrix}$$

$$= \begin{bmatrix} x_b c\alpha c\beta + y_b(c\alpha s\beta s\gamma - s\alpha c\gamma) + z_b(c\alpha s\beta c\gamma + s\alpha s\gamma) + \Delta x \\ x_b s\alpha c\beta + y_b(s\alpha s\beta s\gamma + c\alpha c\gamma) + z_b(s\alpha s\beta c\gamma - c\alpha s\gamma) + \Delta y \\ -x_b\, s\beta + y_b\, c\beta\, s\gamma + z_b\, c\beta\, c\gamma\ + \Delta z \\ 1 \end{bmatrix} \tag{5}$$

where $(\Delta x, \Delta y, \Delta z)$ are the displacement of origin of frame {J} with respect to frame {B} and roll (α), pitch (β), and yaw (γ), represents the rotations of frame {J} with respect to frame {B}. Using equation 5, we can mathematically track the deviation of every point on the cutting path from its ideal position on the bone to its corresponding point on the cutting guide based on the change in position of the guide. The error in positioning (e) is calculated as the scalar displacement of the ideal cutting path the bone from the path designed on the guide.

$$e = |\vec{\mathbf{e}}| = \left|\vec{\mathbf{r}}_j\ -\ \vec{\mathbf{r}}_b\right|$$

For example,

If frame {J} has a roll of 30 degrees (α)and pitch of 60 degrees (β) and is translated 5 units in $\hat{Z}_B$ (Δx). If the point represented by the position vector $\vec{\mathbf{r}}_b = [1\ 1\ 0]^{\mathrm{T}}$ in frame {B}. If $\vec{\mathbf{r}}_j$ is the position vector of the same point from frame {J}, then using equations 1 & 5 we have,

$$ {}^{J}_{B}\mathbf{H} = \begin{bmatrix} 0.433 & -0.250 & 0.750 & 0.000 \\ 0.250 & 0.866 & 0.433 & 0.000 \\ -0.866 & 0.000 & 0.500 & 5.000 \\ 0 & 0 & 0 & 1 \end{bmatrix} \tag{6} $$

$$ \vec{\mathbf{r}}_j = {}^{J}_{B}\mathbf{H}\,\vec{\mathbf{r}}_b = {}^{J}_{B}\mathbf{H} \begin{bmatrix} 1.0 \\ 1.0 \\ 0.0 \\ 1.0 \end{bmatrix} = \begin{bmatrix} 0.18 \\ 1.12 \\ 4.13 \\ 1.0 \end{bmatrix} \tag{7} $$

The error vector $\vec{\mathbf{e}}$ is the difference between the two vector $\vec{\mathbf{r}}_j$ and $\vec{\mathbf{r}}_b$, expressed as,

$$ \vec{\mathbf{e}} = \vec{\mathbf{r}}_j - \vec{\mathbf{r}}_j = \begin{bmatrix} \mathbf{0.18} \\ \mathbf{1.15} \\ \mathbf{4.13} \\ \mathbf{1.0} \end{bmatrix} - \begin{bmatrix} \mathbf{1.0} \\ \mathbf{1.0} \\ \mathbf{0.0} \\ \mathbf{1.0} \end{bmatrix} = \begin{bmatrix} \mathbf{-0.82} \\ \mathbf{0.12} \\ \mathbf{4.134} \\ \mathbf{0.0} \end{bmatrix} \tag{8} $$

The scalar error, *e*, is defined as the magnitude of the vector

$$ e = |\vec{\mathbf{e}}| = \mathbf{4.21}\ mm \tag{9} $$

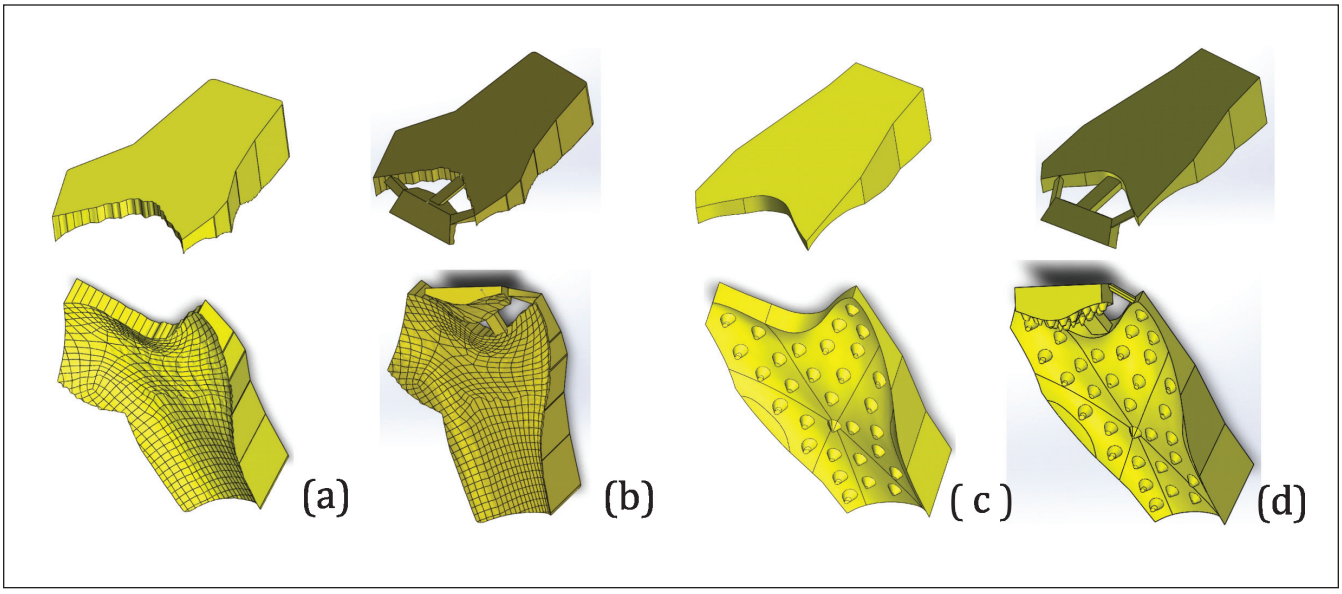

Figure E: Different types of guides used in positioning experiment (a) standard with no features, (b) standard with a gusset, (c) surface with distributed spikes, and (d) surface with distributed spikes and gusset.

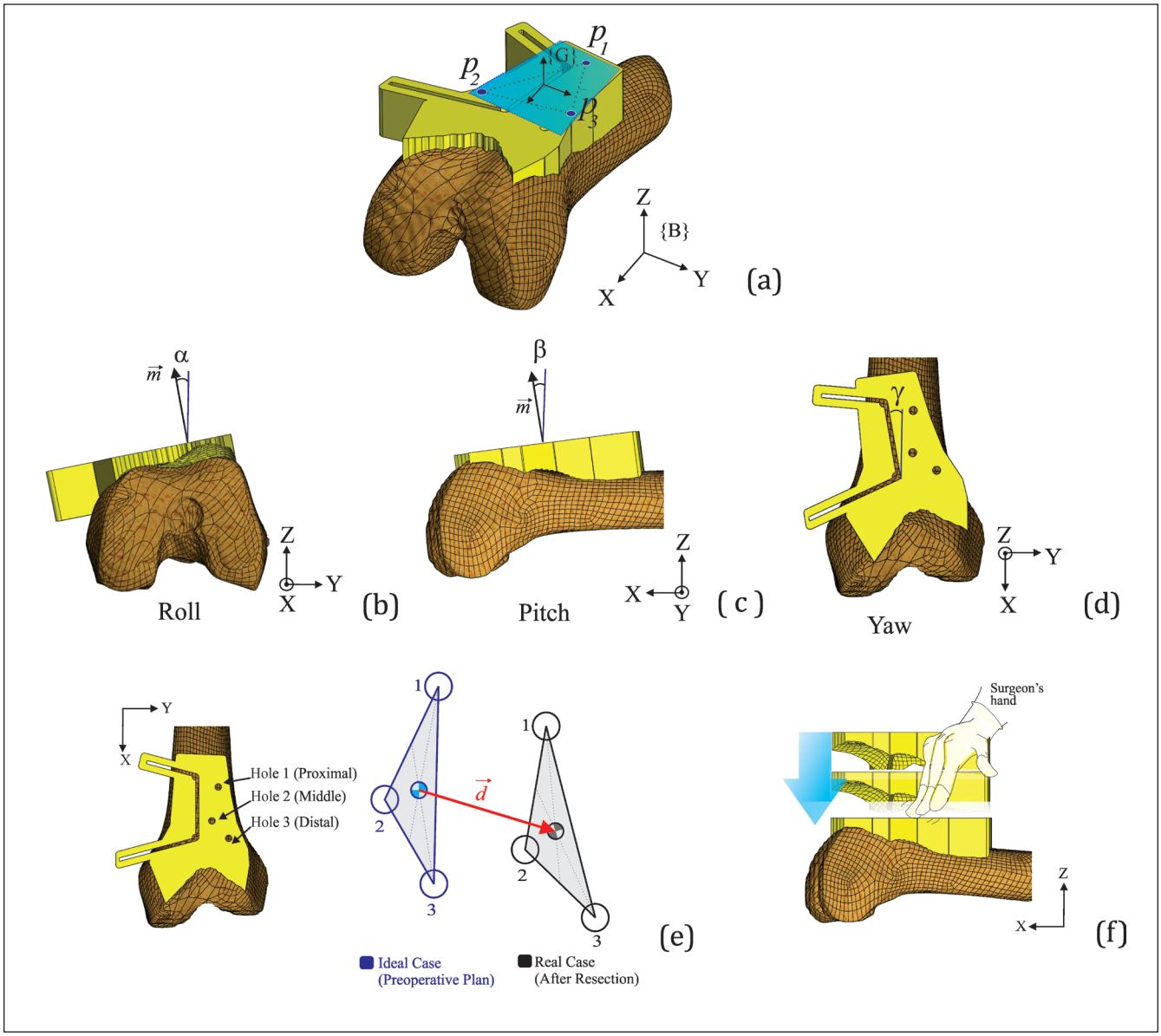

Figure F: (a) Calculating rotations of cutting guide after positioning by defining a plane as a reference using three fiducial points: P1, P2, and P3 from the top surface of cutting guide; (b, c, & d) calculation of angles of roll (α), pitch (β), and yaw (γ); (e) Calculating the X and Y translations of the cutting guide before and after the placement of guide on surface of the bone, using CT-scans and Steinmann pin holes and (f) Translation of cutting guide along the Z axis, surgeon presses the guide on the surface of the bone prior to the resection.